Lawrence Berkeley National Laboratory

Recent Work

Title
COAL LIQUEFACTION RESEARCH SEMI ANNUM, REPORT. OCT. 1, 1930 TO MARCH 30, 1981.

Permalink
https://escholarship.org/uc/item/7m4010h3

Author
Heinemann, H.

Publication Date
1981-03-01

Lawrence Berkeley Laboratory
UNIVERSITY OF CALIFORNIA

Materials & Molecular Research Division

COAL LIQUEFACTION RESEARCH
SEMI ANNUAL REPORT
October 1, 1980 to March 30, 1981

Heinz Heinemann

March 1981

DISCLAIMER

SEMI ANNUAL REPORT

October 1, 1980, to March 30, 1981

COAL LIQUEFACTION RESEARCH

Principal Investigator: Heinz Heinemann

Lawrence Berkeley Laboratory

University of California

Berkeley, CA 94720

This manuscript was printed from originals provided by the author.

Principal Investigator: Heinz Heinemann

Lawrence Berkeley Laboratory

University of California

Berkeley, CA 94720

This project is aimed at examining the differences between Fischer-Tropsch reactions carried out in a slurry reactor on the one hand and in a fixed bed reactor on the other hand. As outlined in our previous report, there are two differences between slurries and fixed beds: 1) in a slurry reactor, less catalyst deactivation is observed, even at low H_2/CO ratios. 2) The product distributions are different: Higher relative amounts of heavy products are produced in the slurry. Both of these differences have been confirmed experimentally. An earlier phase of this project was concerned with temperature control in the reactors. (See report of July 10, 1981). The present phase centers on an investigation of mass transport phenomena. We are engaged in research on two levels: experimental and computational.

A. Experimental work

The experiments have been aimed at measuring mass transfer coefficients and reaction kinetics, which will be used in a model of the slurry reactor. Obtaining data has been difficult, for two mechanical reasons. First, the flow controllers have not been functioning properly, and second, the catalyst tends to cake, and sometimes plug the reactor. Experiments with a glass column, the geometry of which is similar to that of the pressure slurry reactor have led to the design of baffles that break up clumps of catalyst.

The data we have taken allow us to draw some conclusions about the Fischer-Tropsch slurry system. Using the apparatus described in the report of September 26, 1980, the rates of production of CO_2 and hydrocarbons through C_{10} were measured as a function of H_2/CO ratio and temperature. The catalyst was subjected to six days of reduction under 10 atm of hydrogen at a space velocity of 80 CM^3/min-g catalyst. The catalyst loading was .125 of catalyst/g slurry liquid. The data discussed here were taken over a ten-day period. A schedule of the run is shown in Table 1. After the first 50 hours, no deactivation was observed. The data shown were all taken during steady state operation. Table 2 shows rates of production of CO_2 and hydrocarbons through C_{10} as a function of temperature, at H_2/CO = .96 and P = 10 Atm. If no water is produced, the rate at which carbon is incorporated into hydrocarbons will be equal to the rate of CO_2 production. The total rate of carbon incorporation through C_{10} is shown in the last column in Table 2. If this rate is lower than the rate of CO_2 production, some of the

CO is consumed to make other products. The fate of this CO is not known. It may form surface carbon; it may react with the iron to make iron carbide; it may react with the slurry liquid; or it could make alcohols, which were present in small amounts. It is also possible that the CO is converted to heavier hydrocarbons, which stay in the slurry liquid. If the rate of carbon incorporation into hydrocarbons is greater than the rate of CO_2 production, hydrogen must react on the catalyst surface to produce water. From the numbers in Table 2, it can be seen that at low temperature, water is produced. This is consistent with the equilibrium behavior of the water gas shift reaction: low temperature favors the production of water. (1). As temperature increases, the rate of consumption of CO for other products increases. This is consistent with McKee's (2) data on fixed bed reactors, which showed that carbon formation increased with temperature.

In Figure 1, activation energy plots are shown for CO_2, CH_4, and C_2H_4. All of the curves show activation energies that decrease as temperature increases, although they remain relatively high. (31 K cal for CO_2) This is an indication that mass transfer is starting to affect the rate of reaction. The mass transfer resistance appears to be at the gas-liquid interface: Calculations based on published correlations for $k_L a$ (3) and the measured rate of reaction at 300°C predict a slight concentration difference between the gas-liquid interface and the catalyst surface. Further, calculations based on the measured rate, using the correlation presented by Satterfield (4), show that under the conditions used, the reaction is far from an internal diffusion limited regime.

Figure 2 shows the product distribution as a function of temperature. The changes in product distribution, while not large, are consistent with other work in fixed beds. $\frac{C_n}{C_1}$ for a given n, decreases as temperature increases; light products are favored at high temperature.

Rates of reaction as a function of H_2/CO ratio are shown in Table 3. Again, the total rate of carbon consumption is shown. In every case, a significant amount of CO is reacting to produce something other than C_1 through C_{10} hydrocarbons. The fraction f of CO that goes to other products is given by $f = 1 - \frac{\Sigma\, nR_{cn}}{R_{CO_2}}$

f is not a strong function of H_2/CO; however, as we might expect, f increases as the H_2/CO ratio decreases.

The product distribution as a function of H_2/CO ratio is also shown in Figure 3. As the H_2/CO ratio increases, the curve $\frac{C_n}{C_1}$ vs. n becomes steeper; lighter products are favored.

Note that the rates of reaction at 300°C and H_2/CO = .88 are significantly different from those at H_2/CO = .96 and 300°C. This is believed to result from a higher degree of carbidization at H_2/CO = .96. As shown in Table 1, the data at H_2/CO = .88 was taken after a long period of

running at high H_2/CO ratio. The higher value for f at $H_2/CO = .88$ supports this hypothesis: since the catalyst is less carbided, the rate of carbon consumption for carbiding increases.

B. Computational Work

A model for the slurry reactor has been developed, assuming plug flow in the gas, and a well-stirred liquid phase. Such a model gives rise to a differential mass balance equation for each component in the gas phase, an overall balance for the gas phase, and in integral balance for each component in the liquid phase. In the equations presented, all variables are defined in the nomenclature section on page 9 .

The gas phase balance is:

$$\frac{-d^{U C_i}}{dz} = k_L a_i \left(\frac{C_i}{H_i} - C_{iL}\right) \tag{1}$$

The overall balance comes from summing equation (1) over all components:

$$- \frac{du}{dz} = \frac{1}{c_{TOT}} \sum_{i=1}^{n} \frac{k_L a_i}{H_i} (C_i - C_L i) \tag{2}$$

The liquid phase balance can be written:

$$Q_L C_{iL} + \int_0^{V_R} R_L a_i \left(\frac{C_i}{H_i} - C_{iL}\right) d V_R - R_i V_R = 0 \tag{3}$$

Rearranging the integral yields:

$$- Q_L C_{iL} + \frac{V_R k_L a_i}{H_i} \left(\overline{C_i} - C_{iL} H_i\right) - R_i V_R = 0 \tag{4}$$

where $\overline{C_i} = \frac{1}{L} \int_0^L C_i d_z$

these equations are solved in the following manner:

1) Guess C_{iL}

2) Solve the gas phase mass balances

3) Evaluate $\overline{C_i}$

4) Check to see if the liquid balance is satisfied·

5) If not, go to 1) and guess a new C_{iL}

A Fortran program has been written to find this solution, and has been tested on the simple case: $2 CO + 2H_2 \longrightarrow CO_2 + CH_4$, where the reaction is assumed to be first order in H_2 and zero order in CO. The differential equation solvers on file at U.C. is used to solve the gas phase balances, and the regula falsi method is used to iterate C_{iL}. The regula falsi method has been found to converge.

The work proposed in the immediate future remains, for the most part, unchanged. We will continue to look at mass transfer effects, and the extent to which recombination occurs: both can have an effect on deactivation and product distribution. However, the work presented here may indicate that deactivation is different in the slurry reactor, regardless of heat or mass transfer. The presence of the slurry liquid may change the course of the reaction on the catalyst surface.

Table 1

Schedule of the Run Reported Here

Time, Hours	Conditions
0-57	$H_2/CO = 1.0$
	$T = 300^o C$
57-76	$H_2/CO - 1.0$
	$T = 270^o C$
76-95	$H_2/CO = 1.0$
	$T = 285^o C$
95-100	$H_2/CO = 1.0$
	$T = 320^o C$
100-121	$H_2/CO = 1.0$
	$T = 300^o C$
121-165	$H_2/CO = 3.0$
	$T = 300^o C$
165-200	$H_2/CO = 2.0$
	$T = 300^o C$
200-213	$H_2/CO = .88$
	$T = 300^o C$
213-235	$H_2/CO = .374$
	$T = 300^o C$
235-240	$H_2/CO = 1.0$
	$T = 300^o C$

TABLE 2

$H_2/CO = .96$

Rates in moles/min-g catalyst

T	R_{CO_2} $\times10^4$	R_{CH_4} $\times10^5$	$R_{C_2}^=$ $\times10^5$	R_{C_2} $\times10^6$	$R_{C_3}^=$ $\times10^6$	R_{C_3} $\times10^7$	$R_{C_4}^=$ $\times10^6$	R_{C_4} $\times10^7$	$R_{C_5}^=$ $\times10^6$	R_{C_5} $\times10^7$	$R_{C_6}^=$ $\times10^6$	R_{C_6} $\times10^6$	$R_{C_7}^=$ $\times10^6$	R_{C_7} $\times10^7$	$R_{C_8}^=$ $\times10^6$	R_{C_8} $\times10^7$	$R_{C_9}^=$ $\times10^6$	R_{C_9} $\times10^7$	$R_{C_{10}}^=$ $\times10^6$	$R_{C_{10}}$ $\times10^7$	$\Sigma n R_n$ $\times10^4$
270°C	.144	.297	.106	.179	.67	2.15	.51	.787	.357	1.006	.286*		.153	.433	.203	.443	.175	.390	.131	.318	.213
285°C	.462	.657	.229	.343	-	-	1.275	1.41	.790	1.82	.597*		.427	.827	.427	.820	.399	.907	.302	.663	-
300°C	.833	1.32	.343	.770	2.53	3.53	2.20	3.09	1.45	2.84	.867*		.774	1.31	.674	1.17	.568	1.12	.414	.812	.780
320°C	1.70	2.38	.577	1.17	4.53	5.23	2.98	4.06	2.18	3.95	1.15*		1.49	3.07	1.40	2.54	1.12	2.09	.667	1.16	1.28

$*(R_6 + R_6^=) \times 10^6$

$R^=$ Denotes Rates of Olefin Formation
R Denotes Rates of Paraffin Formation

TABLE 3

T = 300°C; Rates in Moles/Min. g Catalyst

H_2/CO	R_{CO_2}	R_{CH_4}	$R_{C_2^=}$	R_{C_2}	$R_{C_3^=}$	R_{C_3}	$R_{C_4^=}$	R_{C_4}	$R_{C_5^=}$	R_{C_5}	$R_{C_6^=}$	R_{C_6}	$R_{C_7^=}$	R_{C_7}	$R_{C_8^=}$	R_{C_8}	$R_{C_9^=}$	R_{C_9}	$R_{C_{10}^=}$	$R_{C_{10}}$	$\Sigma n R_n$
	$\times10^4$	$\times10^5$	$\times10^5$	$\times10^6$	$\times10^6$	$\times10^6$	$\times10^6$	$\times10^6$	$\times10^6$	$\times10^7$	$\times10^6$	$\times10^7$	$\times10^7$	$\times10^7$	$\times10^7$	$\times10^7$	$\times10^7$	$\times10^8$	$\times10^8$	$\times10^8$	$\times10^4$
2.953	2.410	3.54	1.00	2.61	9.2	1.45	4.9	1.00	2.75	6.8	1.43	3.38	9.60	2.27	5.57	1.30	2.90	7.43	8.33	1.88	1.62
2.00	2.79	2.84	1.04	2.31	9.17	1.64	4.87	.795	2.94	8.37	1.64	4.38	12.3	2.41	8.03	1.69	5.67	12.90	12.02	2.32	1.66
.881	1.54	1.31	.507	.84	3.60	.577	2.73	.399	2.02	4.33	*1.55		9.10	1.57	6.57	1.10	3.99	7.90	15.7	2.79	.913
.374	.697	.597	.259	.246	1.73	.105	1.44	.125	.930	2.43	*.524		4.10	.620	2.72	.457	1.70	2.79	3.42	.426	.403

$*(R_C + R_6^=)$

(1) Newsome, D. S., Catalysis Reviews - Sci. Eng., 21, 275-318 (1980)

(2) McKee, W. G., M. S. Thesis, University of California, Berkeley, Department of Chemical Engineering. (1980)

(3) Kolbel, H., and Ralek, M., Cat. Rev., 21, 225 (1980)

(4) Satterfield, C., Mass Transfer in Heterogeneous Catalysis, MIT Press, 1970.

(5) Cannella, W., and Bell, A. T., Unpublished Results.

(6) Calderbank, P. H., Evans, F., Farley, R., Jepson, G., and Poll, A., Catalysis in Practice, London, Instn. Chem. Engrs. (1963).

NOMENCLATURE

a   Bubble area per reactor volume, cm^{-1}

C_i Gas phase concentration of component i, $moles/cm^3$

C_{iL} Liquid phase concentration of component i, $moles/cm^3$

C_T Total gas phase concentration, $moles/cm^3$

H_i Henry's law constant for component i, $\dfrac{(moles/cm^3)_{gas}}{(moles/cm^3)_{liquid}}$

k_{Li} Mass transfer coefficient for component i from gas-liquid interface to bulk liquid, cm/sec

L   Height of the reactor, cm

R_i Rate of consumption of component i per reactor volume, $moles/sec\text{-}cm^3$

Q_L Volumetric flow rate of liquid, cm^3/sec

V_R Volume of the reactor

k_i rate constant, $\dfrac{moles\ i}{cm^3 sec}\dfrac{(moles\ H_2)^{-1}}{cm^3}$

z   Position in the reactor, cm

ACTIVATION ENERGY PLOT
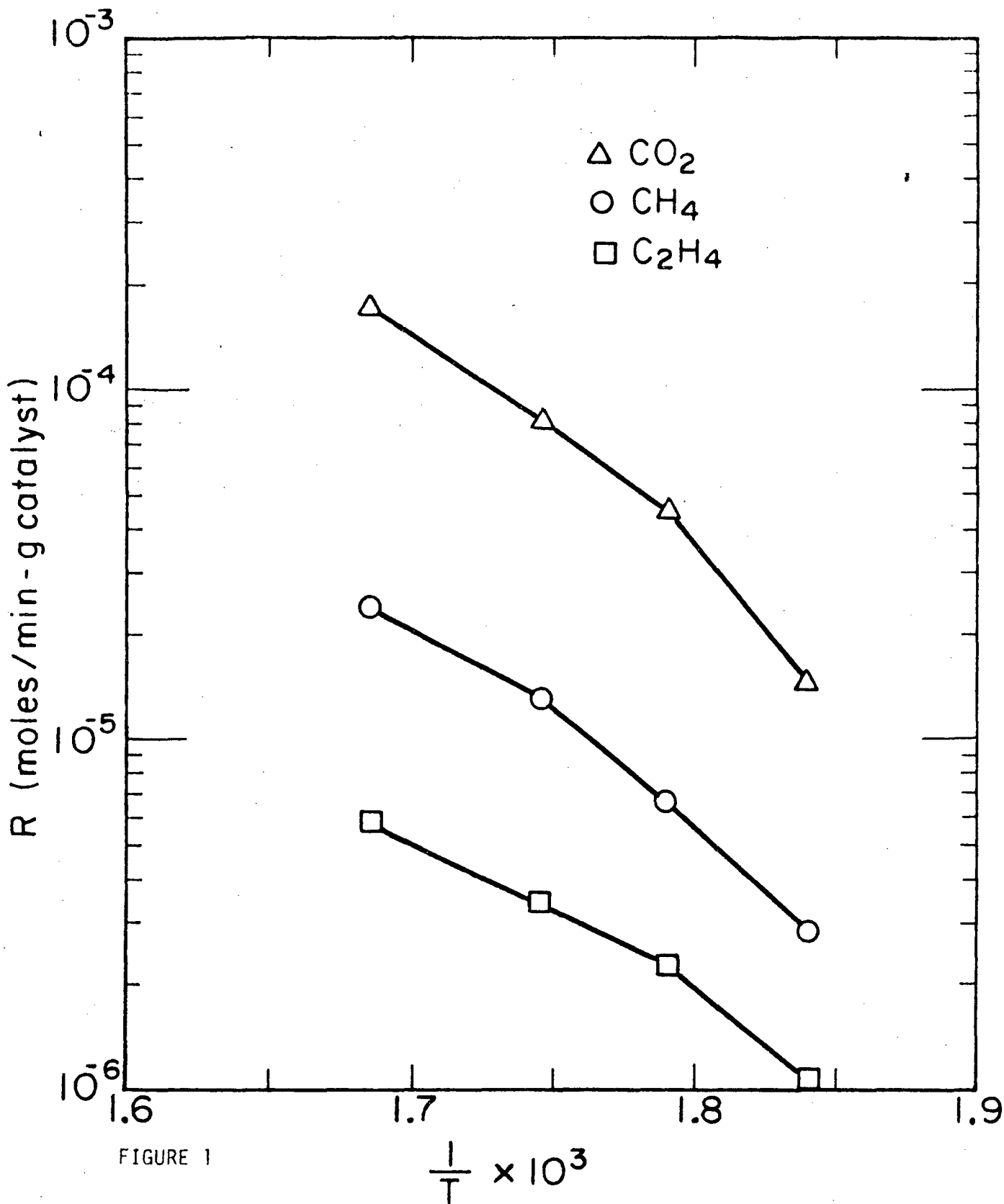
FIGURE 1

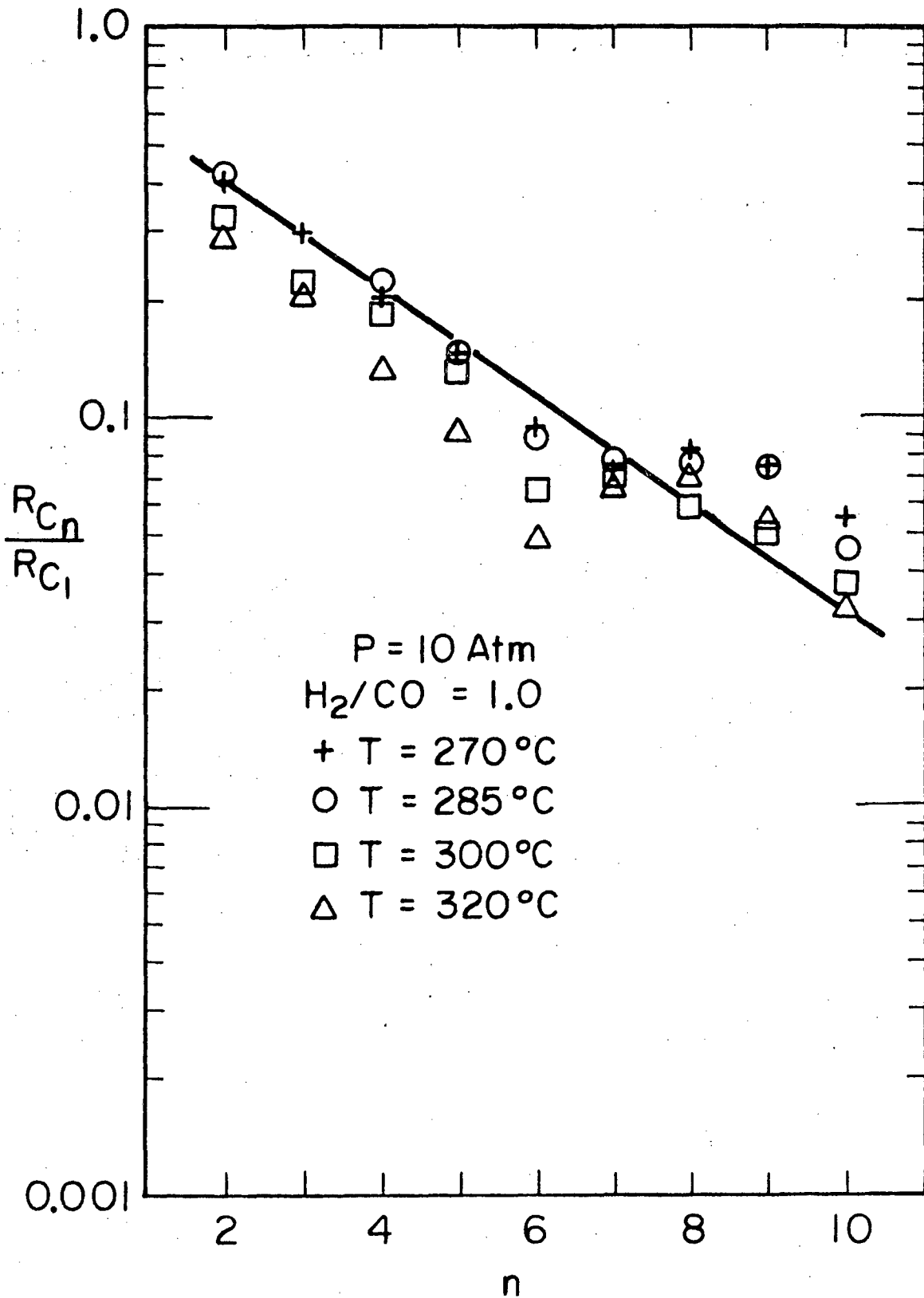XBL 814-3769

EFFECT OF TEMPERATURE ON PRODUCT DISTRIBUTION

FIGURE 2   XBL 814-3770
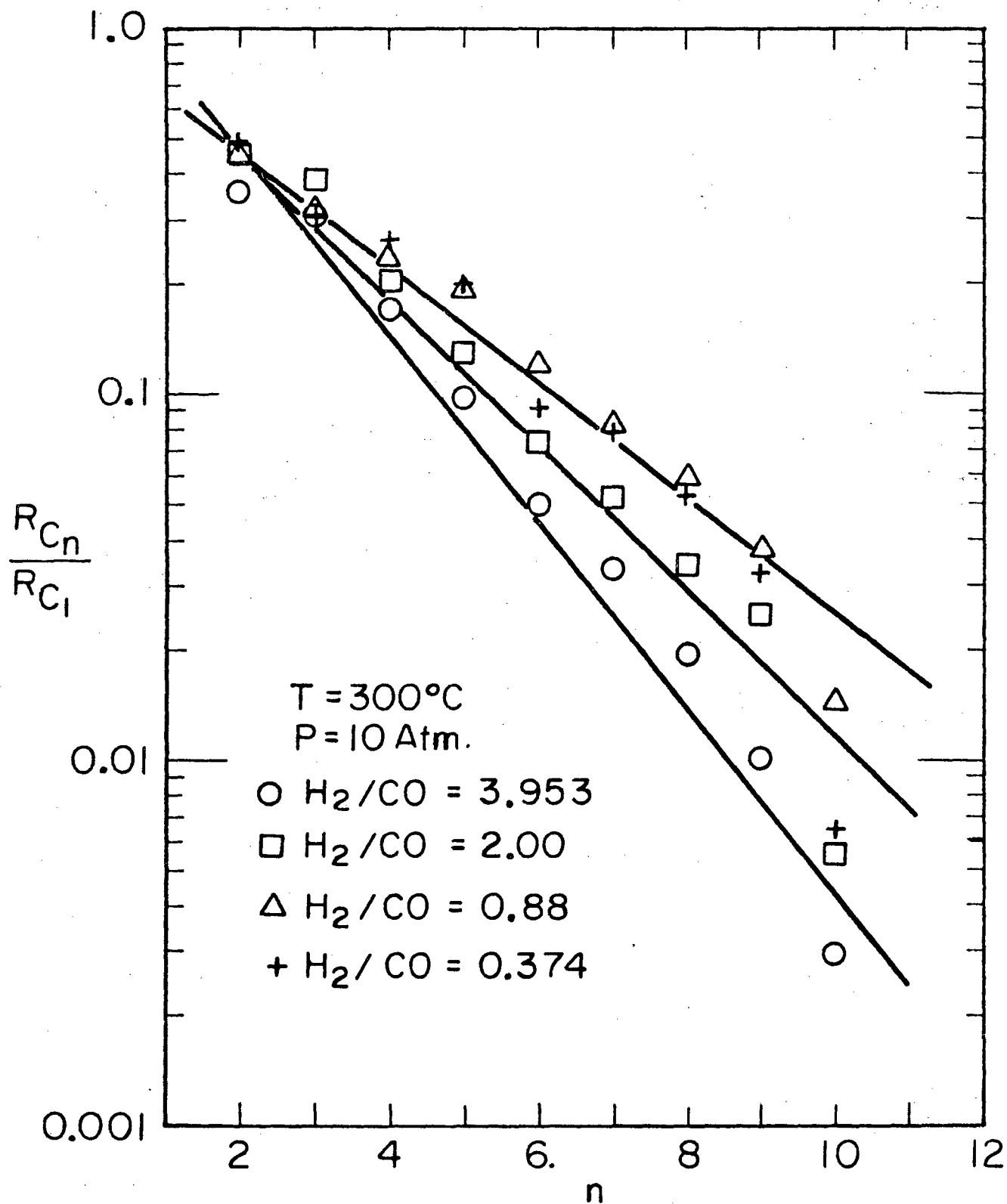
EFFECT OF H_2/CO RATIO ON PRODUCT DISTRIBUTION

$$T = 300°C$$
$$P = 10 \text{ Atm.}$$
$$\bigcirc \quad H_2/CO = 3.953$$
$$\square \quad H_2/CO = 2.00$$
$$\triangle \quad H_2/CO = 0.88$$
$$+ \quad H_2/CO = 0.374$$

FIGURE 3

XBL 814-3767